

# EXPERIMENTAL STUDY OF INTERFACIAL INSTABILITY IN ALUMINIUM REDUCTION CELLS

PEDCENKO, A.<sup>1,2</sup>, MOLOKOV, S.<sup>1,2</sup>, THOMAS, P.J.<sup>2</sup>, LUKYANOV, A.<sup>3</sup>, PRIEDE, J.<sup>1,2</sup>

<sup>1</sup>*Applied Mathematics Research Centre, Coventry University, Priory Street, Coventry, CV1 5FB, UK; [a.pedcenko@coventry.ac.uk](mailto:a.pedcenko@coventry.ac.uk), [s.molokov@coventry.ac.uk](mailto:s.molokov@coventry.ac.uk); [j.priede@coventry.ac.uk](mailto:j.priede@coventry.ac.uk)*

<sup>2</sup>*Fluid Dynamics Research Centre, School of Engineering, University of Warwick, Coventry, CV4 7AL, UK; [pjt1@eng.warwick.ac.uk](mailto:pjt1@eng.warwick.ac.uk)*

<sup>3</sup>*Department of Mathematics, University of Reading, Whiteknights, PO Box 220, Reading, Berkshire, UK; [a.lukyanov@reading.ac.uk](mailto:a.lukyanov@reading.ac.uk)*

**Abstract:** Preliminary results of laboratory study of magnetohydrodynamic instabilities in aluminium reduction cells are presented. The onset of instability, its frequency and amplitude have been measured with electric potential probes and with optical camera. Reconstruction of electric potential inside the liquid metal shows good qualitative agreement with the instabilities observed in real reduction cells.

## 1. Introduction

Understanding the nature of magnetohydrodynamic (MHD) instabilities in aluminium reduction cells is an issue of great importance. Up to now most studies of the phenomenon have been theoretical [1]-[12], see also a review in [13]. Borisov et al [14] reported certain results on experimental study of the MHD instabilities, but the paper lacks any details. Sele [1] presented a mechanism of interfacial instability in the cells, which is based on the interaction of the horizontal disturbance current within the aluminium layer with the vertical background magnetic field. This resulted in a tilted interface rotating counter-clockwise. Here we present preliminary experimental results of the phenomenon which are in qualitative agreement with theoretical predictions by Sele [1] and with more detailed analysis in [4], [6].

## 2. Experimental setup

Experimental setup (Fig. 1) comprises a rectangular box, or cell of 30×30 cm<sup>2</sup> horizontal cross-section having electrically conducting top and bottom and non-conducting, 15 cm high sidewalls. The box is partially filled with liquid metal, In-Ga-Sn alloy. A DC electric current is supplied from the top of the container (anode plate) to its bottom (cathode plate) through the liquid metal layer. The electrolyte layer, which is normally located on top of aluminium layer in industrial cells is replaced by a system of vertical electrodes as described below.

Each electrode is Ø2 mm, 10 mm long, and is made of stainless steel. 900 of such electrodes are uniformly distributed along the 10mm-thick anode plate with 10 mm period, and are dipped vertically down into the liquid metal. The ratio of total cross-section of all of the 900 electrodes to the liquid metal surface cross-section is 3% only. The anode plate with the electrodes can be lifted or lowered changing in this way the electrodes' submerging depth into the liquid metal. This 'multi-electrode' approach allows the liquid metal surface to elevate within the air gap between the anode plate and liquid metal (within the length of the electrodes), and at the same time keeps continuity of current from the anode to the cathode.

The electrodynamic properties of such multi-electrode structure are similar to that of electrolyte layer in the industrial cell: it establishes sufficient uniformity of the vertical current along the free surface of the liquid metal if it is undisturbed. If the liquid metal surface

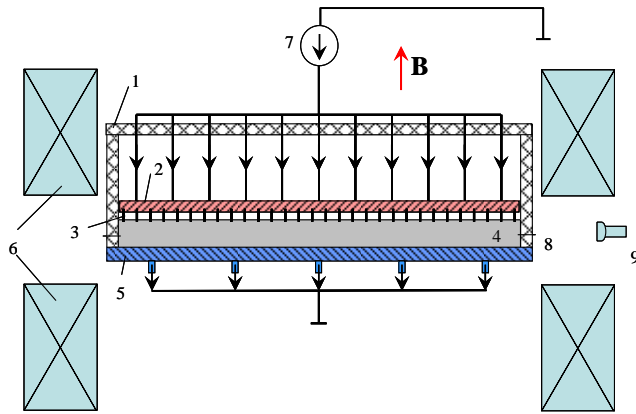


Figure 1. Schematic view of the experimental setup; 1 – plexiglas sidewalls of the cell, 2 – copper anode plate, 3 – stainless steel electrodes, 4 – liquid metal (InGaSn), 5 – steel bottom plate (cathode), 6 – inductor of vertical magnetic field, 7 – current source, 8 – potential probes, 9 – CCD camera.

having vertical current of up to 2 kA, it is room-temperature, and of low electric power consumption.

The bottom of the cell has been made of stainless steel with electrical conductivity of  $\sim 2.5$  times lower than that of the liquid metal. This allows the disturbance electric current to complete its path mainly in the liquid metal rather than in the poorly conducting cathode. Similar path of disturbance current exists in the real cells and this leads to the instability.

The cell is supplied with the DC current from  $3 \times 600\text{A}$  current sources (Magna Power PQ5-600). Special attention has been paid to establishing uniformity of the current through the 900 electrodes by means of connecting the anode plate to the current sources via 100 wires uniformly distributed along its top surface.

The cell with liquid metal has been placed in the vertical, uniform, steady magnetic field generated by the pair of rectangular water-cooled Helmholtz coils, fed with DC current from another two 600A current sources (Magna Power PQ16-600), which provide maximum density of the magnetic flux of  $\sim 100$  mT and of  $\sim 5\%$  maximum non-uniformity of the field's vertical component in the liquid metal volume.

### 3. Experimental procedure and measurement technique

There are three main experimental parameters that are controlled during the tests: the height of the liquid metal level  $h$ , the vertical current strength  $I$  through the liquid metal layer and the density of the magnetic field flux  $B_0$ . Liquid metal height  $h$  has been kept constant during each test run, while magnetic field induction and vertical current strength varied, either by keeping magnetic field at maximum and increasing the current, or the other way around.

The electric current passage from the top of the liquid metal towards the bottom is linked to the distribution of the electric potential inside the liquid metal. The electric potential along the horizontal cross-section correlates with the shape of the liquid metal layer. In the ideal case when the current is distributed uniformly along both top and bottom surfaces of the liquid metal, electric potential value depends only on the vertical coordinate. If the shape of the metal layer changes due to some reason, the electric current in the liquid metal redistributes in the way that provides lowest resistance for its passage. The global distribution of the potential changes as well.

is deformed, it amplifies the current value in the elevated liquid metal areas and lowers it in the shallow ones. The use of 'multi-electrode' anode as a replacement for an electrolyte layer eliminates many undesired side-effects: electrolysis, high Joule losses in the electrolyte, ionic conductivity, high temperatures, necessity of electrolyte cooling and continuous renewal, high chemical aggressiveness of media, necessity to remove the products of the electrolysis including gases, etc. In contrast, multi-electrode 'model of electrolyte' is safe, allows

To register global changes in the electric potential distribution 24 copper electrodes of  $\varnothing 0.5$  mm have been installed in the side-walls of the cell at equal distance from the container's bottom and uniformly distributed along the perimeter of the cell (Fig. 1, pos. 8) with 50 mm period. All the electrodes measured potential difference between their position and the point at the centre of the container's bottom. When the current is switched on, the readings of the probes differ slightly due to the different distances between their locations and the central 'zero' electrode. This static distribution was accounted for by acquiring such 'undisturbed' potential patterns for a certain strength of the electric current and taking reading from each probe afterwards.

The signals from the probes were acquired with 6 'Data Translation DT9821' 24-bit high resolution USB acquisition boards having 4 analog independent inputs each. The typical values of registered signals are 10 mV at 1.2 kA of anode current for the liquid metal surface elevation of a few mm. The signals from all 24 probes were recorded simultaneously with the rate of 120 samples per second and processed by interpolating the acquired data over the whole horizontal cross-section of the liquid metal using Kriging technique. The performance of the acquisition system was tested by artificially inducing gravitational waves in one or another direction in the liquid metal layer.

#### 4. Preliminary results

The onset of the instability is found to depend on the magnitudes of the electric current through the cell  $I$  and on the background DC magnetic field  $B_o$ . First, preliminary series of the experiments were conducted at  $B_o = 30$  mT and liquid metal level of  $h = 2$  cm. Instability manifests itself as liquid metal wave travelling along the perimeter of the cell that can be observed visually as a rotating interface of the liquid metal. The direction of the wave propagation depends on the sign of the background magnetic field: it travels in the counter-clockwise direction for magnetic field pointing upwards, and clockwise if magnetic field points downwards. The amplitude of the disturbed surface elevation observed in the experiments varies between 0 to 10 mm depending on the strength of the vertical current  $I$ . Fig. 2 shows time-evolution of the electric potential in the liquid metal at one of the probes at constant vertical current  $I=160$ A and  $B_o=30$  mT. Figs. 3 and 4 show frequency spectrum of these oscillations with main frequency  $f_o = 0.71$  Hz, as well as the dependence of the amplitude on  $I$ .

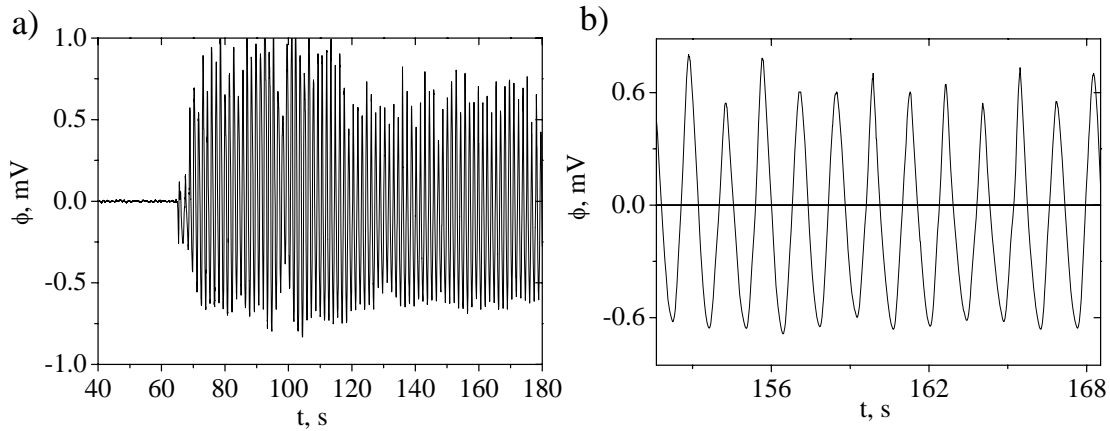


Figure 2 Time-dependent oscillation of the electric potential in the liquid metal: a) the onset of the instability; b) magnified view of the signal in unstable regime.

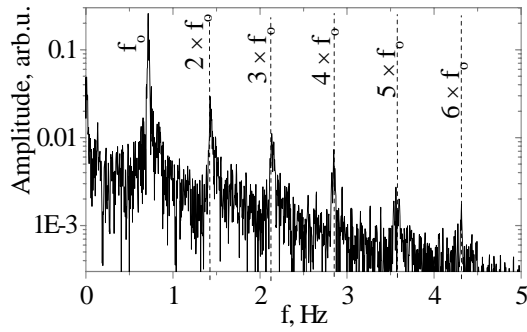


Figure 3 Frequency spectrum of the electric potential oscillations (Fig.3)

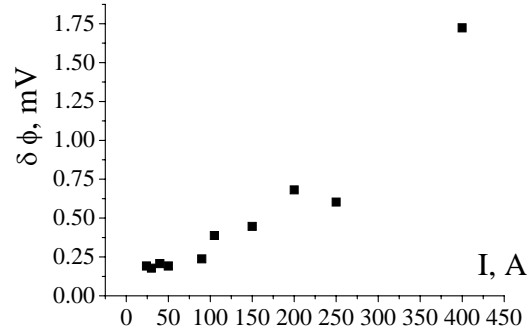


Figure 4 Standard deviation of electric potential oscillations  $\delta\phi$  due to instability wave at different vertical current  $I$  values;  $B_0=30$  mT.

By analysing time-correlations of the potential probes signals acquired at different positions along the perimeter of the liquid metal it is possible to reconstruct time-evolution of the electric potential field. Fig. 5 represents time-series of electric potential maps reconstructed with 0.1 s intervals, which clearly demonstrates a counter-clockwise rotating wave in agreement with theoretical predictions.

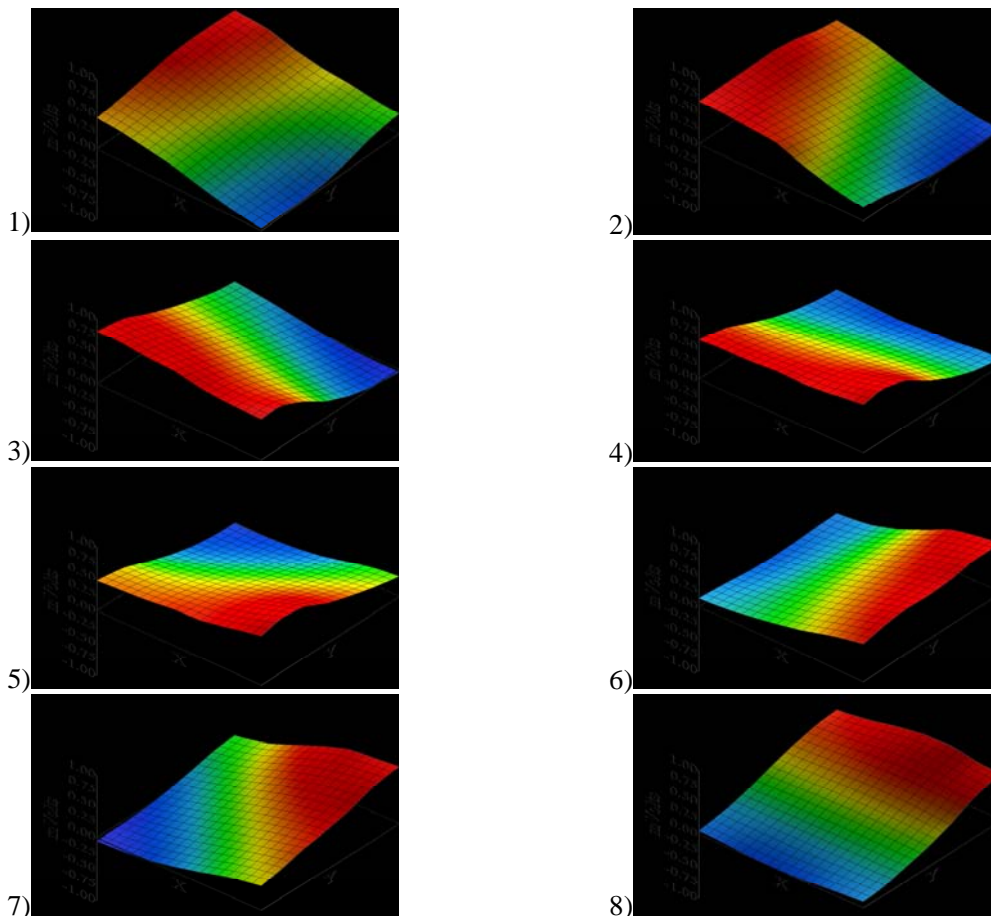


Figure 5 Time-evolution of the electric potential in the liquid metal recorded with potential probes along the perimeter of the cell during propagation of instability wave. Here time interval between frames is 0.13 s;  $I = 80$  A,  $B_0 = 30$  mT,  $h = 2$  cm. The wave propagates counter-clockwise.

## 5. Conclusions

The results show that the replacement of electrolyte layer, which is normally located on top of liquid metal, with a system of vertical electrodes is a viable method to study instabilities relevant to aluminium reduction cells experimentally. This eliminates electrolysis and many other undesired effects with it, such as excessively high Joule heating, production of hazardous gases, etc. This also allows to operate with much higher electric currents at room temperature, and thus to study various phenomena related to aluminium reduction cells in a laboratory.

As expected, the results of the experimental study presented here show that instability appears due to interaction of the horizontal currents in the liquid metal layer and the vertical background magnetic field. The threshold of instability is lower for i) lower thickness of the liquid metal layer,  $h$ , ii) higher vertical current,  $I$ , iii) higher background magnetic field,  $B_0$ . The detailed experimental results and comparison with the theoretical predictions is in progress. They will be presented in a full journal paper.

**Acknowledgement:** The authors are indebted to Carbon Trust, Alcan International, Applied Mathematics Research Centre of Coventry University and Fluid Dynamics Research Centre of University of Warwick for financial support of this study.

## References

- [1] Sele, T.: Metallurgical Transactions 8B (1977) 613-618
- [2] Urata, N.: Light Metals (1985) 581-591
- [3] Lukyanov, A.; El, G.; Molokov, S.: Phys. Lett. A., 290 (2001) 165-172
- [4] Molokov, S.; El, G.; Lukyanov, A.: Coventry University, AMRC Internal Report AM-01/2003 (2003)
- [5] Kohno, H.; Molokov, S.: Phys Lett A 366 (2007) 600-605
- [6] Kohno, H.; Molokov, S.: Int J Engng Sci 45 (2007) 644-659
- [7] Sun, H.; Zikanov, O.; Ziegler, P.: Fluid Dynamics Research 35 (2004) 255-274
- [8] Davidson, P.A.; Lindsay, R.L.: J. Fluid Mech 362 (1998) 273-295
- [9] Bojarevics, V.; Romerio, M.V.: Eur. J Mech B/Fluids 13 (1994) 33-56
- [10] Bojarevics, V.; Pericleous, K.: Light Metals (2006) 347-352
- [11] Sneyd, A.D.: J Fluid Mech 236 (1992) 111-126
- [12] Sneyd, A.D.; Wang, A.: J Fluid Mech 236 (1994) 111-126
- [13] Gerbeau, J.-F., Le Bris, C., Lelievre: T. Mathematical Methods for the Magnetohydrodynamics of Liquid Metals. Oxford University Press (2006)
- [14] Borisov, I.D.; Poslavskiy, S.A.; Rudnev, Y.I.: XXI ICTAM, 15-21 August 2004, Warsaw, Poland (2004)